



Bragg grating induced cladding mode coupling due to asymmetrical index modulation in depressed cladding fibers

Berendt, Martin Ole; Grüne-Nielsen, Lars; Soccolich, C.F.; Bjarklev, Anders Overgaard

Published in:

Technical Digest Optical Fiber Communication Conference and Exhibit

Link to article, DOI:

[10.1109/OFC.1998.657157](https://doi.org/10.1109/OFC.1998.657157)

Publication date:

1998

Document Version

Publisher's PDF, also known as Version of record

[Link back to DTU Orbit](#)

Citation (APA):

Berendt, M. O., Grüne-Nielsen, L., Soccolich, C. F., & Bjarklev, A. O. (1998). Bragg grating induced cladding mode coupling due to asymmetrical index modulation in depressed cladding fibers. In *Technical Digest Optical Fiber Communication Conference and Exhibit* (pp. 7-8). IEEE. <https://doi.org/10.1109/OFC.1998.657157>

General rights

Copyright and moral rights for the publications made accessible in the public portal are retained by the authors and/or other copyright owners and it is a condition of accessing publications that users recognise and abide by the legal requirements associated with these rights.

- Users may download and print one copy of any publication from the public portal for the purpose of private study or research.
- You may not further distribute the material or use it for any profit-making activity or commercial gain
- You may freely distribute the URL identifying the publication in the public portal

If you believe that this document breaches copyright please contact us providing details, and we will remove access to the work immediately and investigate your claim.

measured phase delay error for a similar but apodized grating. As expected, apodization decreased the ripples.

Although this technique was demonstrated on short commercial gratings, it is better suited to resolve the phase ripples in long dispersion-compensating gratings.

1. S. Barcelos *et al.*, Electron. Lett. 31, 1280 (1995).
2. M. Volanthen *et al.*, Electron. Lett. 32, 757 (1996).
3. K. Takiguchi *et al.*, IEEE Photon. Technol. Lett. 6, 86 (1994).
4. K. Ennsner *et al.*, presented at European Conference on Optical Communication (ECOC'97), Edinburgh, Scotland, 1997.
5. G.H. Smith *et al.*, Electron. Lett. 33, 74 (1997).

TuA6 **12:15pm**

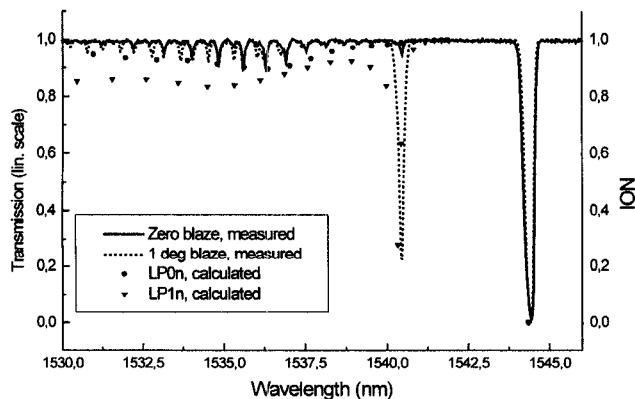
Bragg grating induced cladding mode coupling due to asymmetrical index modulation in depressed cladding fibers

Martin O. Berendt, Lars Grüner-Nielsen,* Carl E. Socolich,** Anders Bjarklev, Department of Electromagnetic Systems, EMI, DTU Building 348, DK-2800 Lyngby, Denmark; E-mail: mob@emi.dtu.dk

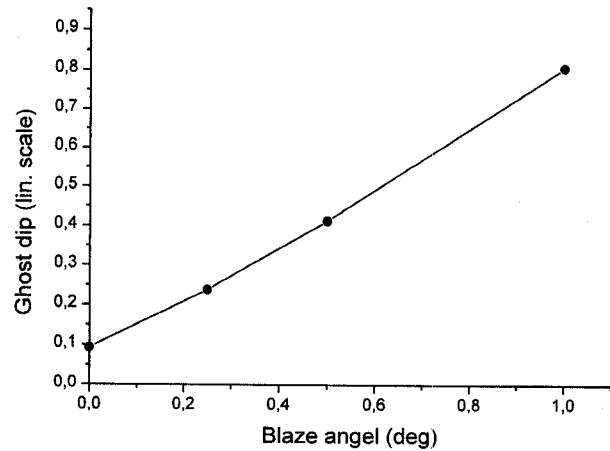
UV-written Bragg gratings find wide spread use as wavelength selective components. In reflection high extinction ratios is routinely obtained. However, coupling to cladding modes gives excess loss on the short wavelength side of the main reflection. Different fiber-designs have been proposed to reduce this problem.¹⁻³ Neither of these designs seems to give complete solutions. In particular, the otherwise promising depressed cladding design gives a pronounced coupling to one LP_{in} mode, this has been referred to as a Ghost grating.⁴

To find the modes of the fiber we have established a numerical modesolver based on the staircase-approximation method. The Bragg grating causes coupling between the fundamental LP₀₁ mode and higher order LP_p modes that satisfy phasematching. The coupling strength is determined by the overlap integral of the LP₀₁, the LP_p mode, and the UV-induced index perturbation. For LP_{on} the index perturbation is set to one in the core and zero elsewhere. For LP_{in} it is simplified to the worst case, *i.e.*, opposite sign of the field.

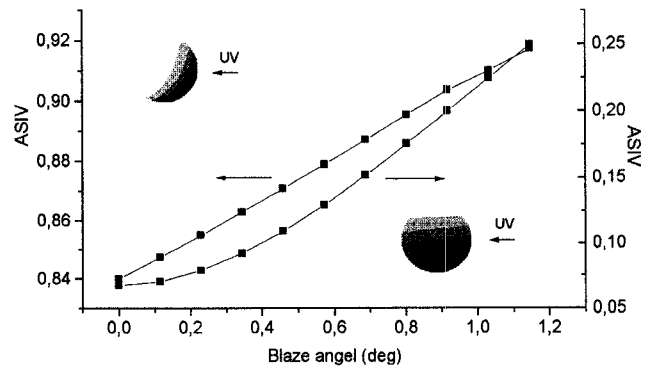
Figure 1 shows measured transmission spectra along with normalized overlap integrals (NOI) calculated for the fiber index profile. The fiber used has a high core index ($15 \cdot 10^{-3}$) and a depressed cladding ring



TuA6 Fig. 1. Measured cladding mode coupling spectra and calculated NOI.



TuA6 Fig. 2. Measured Ghost dip relative to Bragg dip as a function of blaze angle.



TuA6 Fig. 3. Asymmetrical index volume (ASIV) as a function of blaze angle, left trace: 800 dB/mm; right trace: 50 dB/mm (note zero slope for zero blaze). Insert shows distribution of UV-induced index perturbation in a fiber cross section.

of depth $-5 \cdot 10^{-3}$ and width $5 \mu\text{m}$. To fit the measured spectrum the depth of the cladding ring was set to $-6 \cdot 10^{-3}$.

At 1°, blaze of the phasemask a large dip is seen 4 nm from the Bragg wavelength. This corresponds to the calculated LP₁₆, LP₁₇ cladding modes. Changing the depth and width of the depressed cladding ring shifts the Ghost dip to other mode numbers but the size and spectral position is virtually unaltered. When the blaze is reduced to $0^\circ \pm 0.02^\circ$ this dip is reduced to six percent of the Bragg dip. This behavior was further investigated by writing four gratings under identical conditions except for blaze angles [(Fig. 2)].

The UV-induced index change was deduced assuming cosine squared longitudinal index modulation, blaze angle θ and exponential attenuation (coefficient γ) of the UV-beam entering the fiber core from the side;

$$n_{UV}(r, \phi, z, \theta) = n_{UV \max} \cdot \exp(-\gamma(\sqrt{a^2 - (r \cdot \sin(\phi))^2} + r \cdot \cos(\phi))) \cdot \alpha_{Blaze}(r, \phi, z, \theta)$$

$$\alpha_{Blaze}(r, \phi, z, \theta) = \frac{a - r \cdot \sin(\phi)}{2a} \cos^2\left(\frac{\pi}{\Lambda} \cdot z\right) + \frac{a + r \cdot \sin(\phi)}{2a} \cos^2\left(\frac{\pi}{\Lambda} \left(z - \frac{2a}{\tan(\theta)}\right)\right),$$

where $n_{UV,max}$ is the maximum UV-induced index change, Λ is the grating period and a is the core radius.

The volume integral of n_{UV} subtracted a cosine squared index modulation is proportional to the NOI, assuming no radial field variation and step azimuthal variation, in the core. This integral we denote as the asymmetrical index volume (ASIV).

The analysis indicate two regimes [(Fig. 3)], namely a blaze-dominated LP_{in} coupling for small UV attenuation (<100 dB/mm) and a side illumination dominated behavior for large UV attenuation. The measurement in Fig. 2 seems to fall in between these extremes. For the fiber used, we estimate an UV attenuation of 400 dB/mm. Comparing this result with the residual Ghost dip for zero blaze and published measurements of index profiles after UV-sidewriting,⁵ we conclude that asymmetry arising from side illumination is very important for the understanding of LP_{in} coupling. Design of fibers and writing setups, with the aim of reducing cladding mode coupling must be based on this new understanding.

*Lucent Technologies Specialty Fiber Devices, Priorparken 680, DK-2605 Brøndby, Denmark

**Lucent Technologies Specialty Fiber Devices, 700 Mountain Avenue, Murray Hill, New Jersey

1. T. Komukai and M. Nakazawa, in *Proceedings of European Conference on Optical Communication (ECOC'95)*, 1995, pp. 31–34.
2. E. Delevaque, S. Boj, J.F. Bayon, H. Poignant, J. Le Mellot, M. Monerie, P. Niay, P. Bernage, in *Optical Fiber Communication Conference*, Vol. 8 of 1995 OSA Technical Digest Series (Optical Society of America, Washington, D.C., 1995), postdeadline paper PD5.
3. L. Dong, L. Reekie, J.L. Cruz, J.E. Capelen, D.N. Payne, in *Proceedings of European Conference on Optical Communication (ECOC'96)*, 1996, pp. 1.53–1.56.
4. S.J. Hewlet, J.D. Love, G. Meltz, T.J. Basily, W.W. Morey, *Electron. Lett.* **31**, 820–822 (1995).
5. A. Vengsarkar, Q. Zhong, D. Inniss, W.A. Reed, P. Lemaire, S.G. Kosinski, *Opt. Lett.* **19**, 1260–1262 (1994).

TuB

11:00am–12:30pm

Room A2

Vertical Cavity Surface-Emitting Lasers

Connie J. Chang-Hasnain, *University of California–Berkeley, Presider*

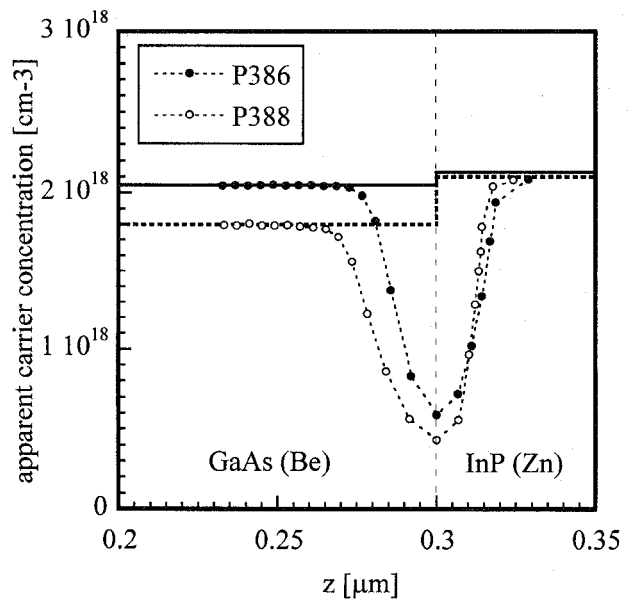
TuB1 (Invited)

11:00am

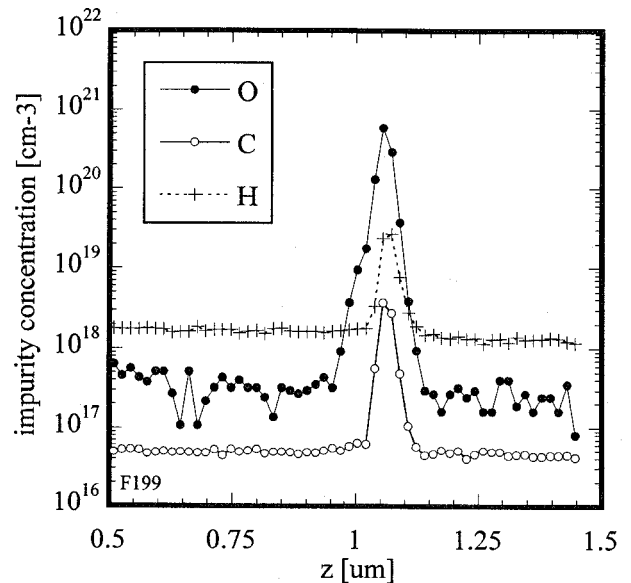
Fusion bonding for vertical-cavity surface-emitting lasers

Dubravko Babić, *Hewlett-Packard Laboratories, Palo Alto, California, 94304; E-mail: babic@hpl.hp.com*

This talk summarizes current efforts in fusion bonding and the application of this technology to vertical-cavity surface-emitting lasers at Hewlett-Packard Laboratories. We discuss electrical characteristics, carrier-concentration profiling and SIMS analyses through InP/GaAs junctions, and the development of 1300 nm VCSELs.



TuB1 Fig. 1. Apparent hole concentration profile in a p -GaAs/ p -InP fused junction.



TuB1 Fig. 2. SIMS profile through a p -InP/ n -GaAs fused junction.